MDPI

(a) Length of growing period (GP) with strong photosynthesis

(b) Day of GP start from Jan 2003 to Dec 2016

(c) Day of GP end from Jan 2003 to Dec 2016

Figure S1. Averaged vegetation phenology achieved using MODIS-EVI (MOD13C1) from 2003-2016, with time resolution of 16 days and spatial resolution of 1x1 degree. It is fitted using combined logistic function. Example of the fitting is shown in Fig 1. Length of growing period (GP), day of start and end of GP in each grid are shown in (a), (b) and (c), respectively.
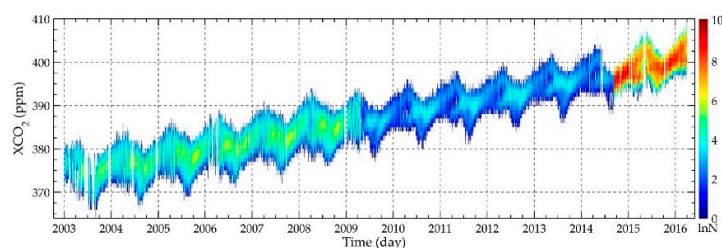

Figure S2. Temporal variation of the all integrated-XCO_2 data points in 30 km/ 8-days from 2003 to 2016. The integrated-XCO_2 is generated by XCO_2 retrievals from SCIAMACHY (2003.01-2009.05), GOSAT (2009.06-2014.08), and OCO-2 (2014.09-2016.03). The plot is color coded by the available number (N) of XCO_2 data points scaled by natural logarithms (lnN).
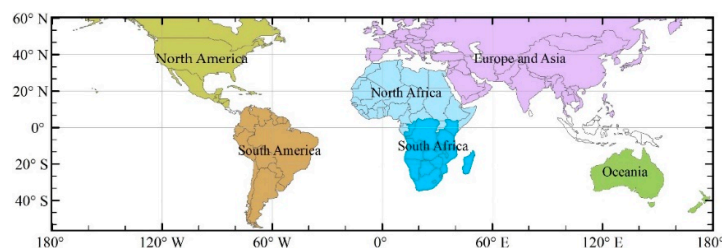

Figure S3. Six regions used for variograms modelling in global mapping XCO_2, which are North America, Eurasia, South America, North Africa, South Africa and Oceania. They are divided by spatial connectivity and different atmospheric transmission between hemispheres.
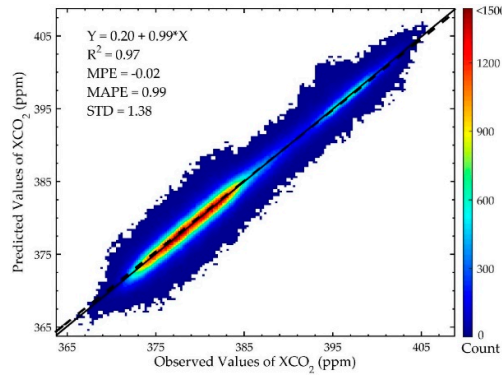
Figure S4. The relation between predicted XCO_2 and integrated-XCO_2 values in cross-validation of global mapping XCO_2 (GM-XCO_2). The color grids represent the density of data distribution. The dotted line is derived from linear regression of predicted values of XCO_2 (Y) and the values of integrated-XCO_2 (X), which shows a significant linear relationship with coefficient of determination (R^2) , 0.97 (p-value < 0.01). And good consistency of integrated-XCO_2 and predicted XCO_2 was shown with mean predicted error (MPE), mean absolute predicted error (MAPE) and standard deviation (STD) equal to -0.02, 0.99 and 1.38 ppm, respectively. The solid line shows the one-to-one line.
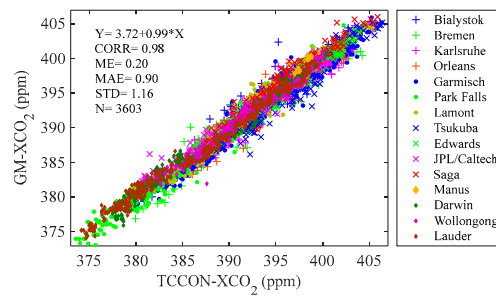

Figure S5. Biases of global mapping XCO_2 (GM-XCO_2) compared with the XCO_2 data derived from 15 TCCON sites within radius of 0.5° in the vicinity of each TCCON site, during January 2003 to March 2016. There are 3603 pairs of grids used in this comparison (GM-XCO_2 minus TCCON XCO_2). Pearson correlation coefficient (CORR), mean bias (ME), mean absolute bias (MAE) and standard deviation (STD) between GM-XCO_2 and TCCON XCO_2 are 0.98, 0.20, 0.90, and 1.16, respectively.

(a) Background GEOS-Chem simulated XCO_2
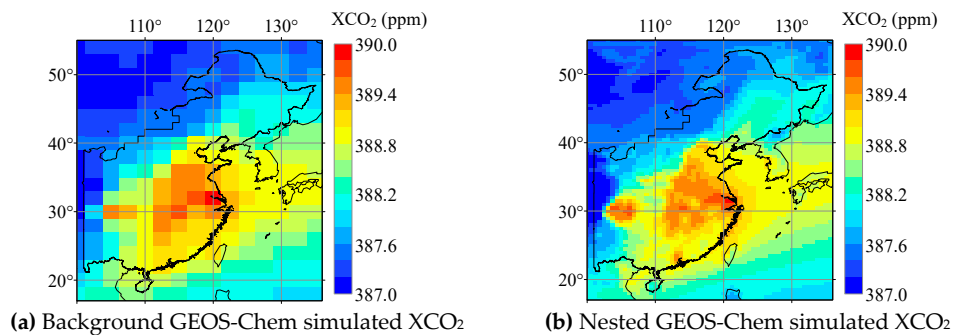
(b) Nested GEOS-Chem simulated XCO_2

Figure S6. Mean values of background (a) and nested (b) GEOS-Chem simulated XCO_2 from 2003 to 2016 over eastern Asia. Spatial resolutions ware 2x2.5 and 0.5x0.625, respectively. Black outline describe the study region, Eastern China.
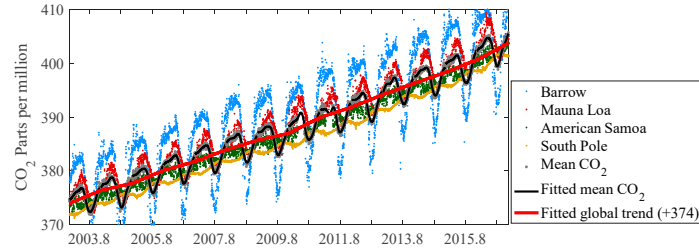
Figure S7. Fitted global trend, using cumulated yearly fitted CO_2 increase, was calculated with data from NOAA (https://www.esrl.noaa.gov/gmd/ccgg/trends/gl_trend.html) and equation (2). Blue, red, green and yellow points are CO_2 data from Barrow, Mauna Loa, American Samoa and South Pole, respectively. Gray points are the averaged values from those four sites' available data. Black line is the yearly fitted result using gray points. The red line is the cumulated yearly fitted trend (+373 ppm). representing fitted global trend.
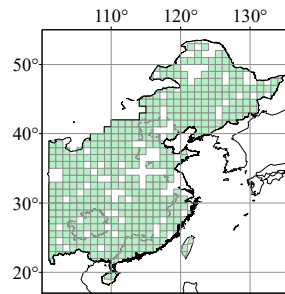

Figure S8. Grids in Eastern China used for VI and XCO_2 trends statistic. It is identified with significant GP, described in section 2.1.2, grids with longitude larger than 100° in China. Area of selected region is $4.47*10^{12}$ m^2, calculated with the grids area from input file of GEOS-Chem model.

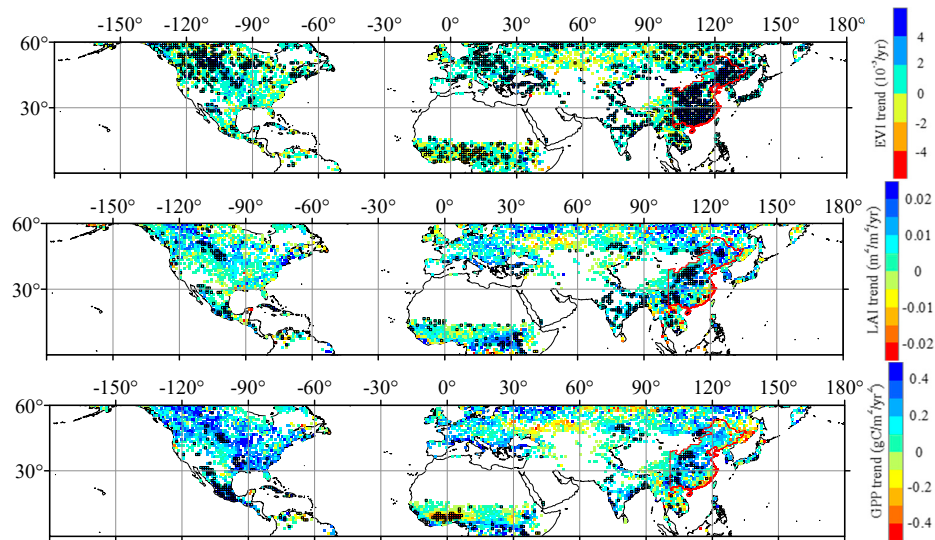**Figure S9.** MODIS EVI increase trends during growing period (GP) (a). MODIS LAI increase trends during GP (b), and MODIS GPP increase trends during GP (c) from 2003 to 2016. Blue grids indicate increasing trends and red grids indicate decreasing trend. Grids with black outlines show the statistical significance (Mann-Kendal test, $p < 0.05$). Study area of eastern China is shown with red edge.
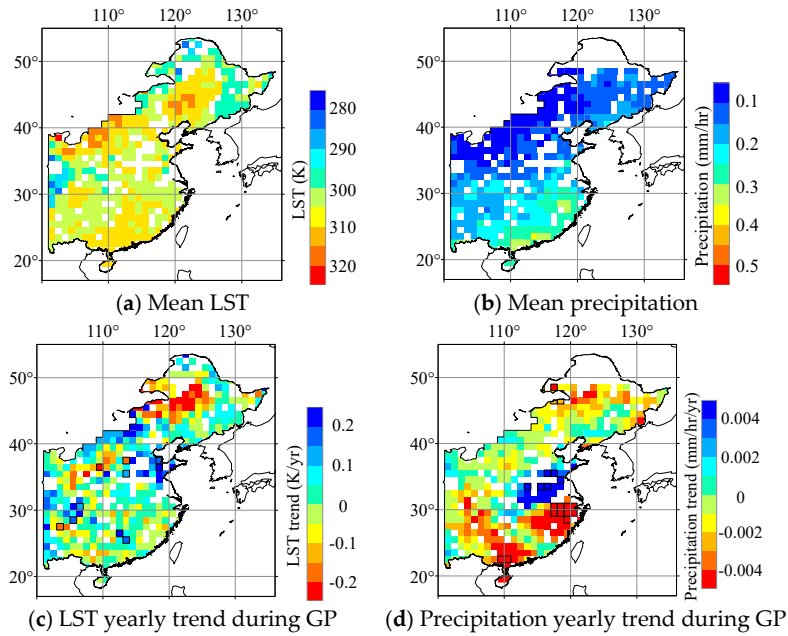
(**a**) Mean LST   (**b**) Mean precipitation

(**c**) LST yearly trend during GP   (**d**) Precipitation yearly trend during GP

Figure S10. Mean land surface temperature (MOD11C2 v6) and precipitation (TRMM 3B42) in growing period from 2003 to 2016 are shown in (a) and (b) respectively. Color bar shows the mean values (blue for low, and red for high). Trends of land surface temperature and precipitation in growing period from 2003 to 2016 are shown in (c) and (d). Color bar shows the trend values (blue for decrease, and red for increase), and black boxes show the significance (Mann-Kendal test, $p < 0.05$).
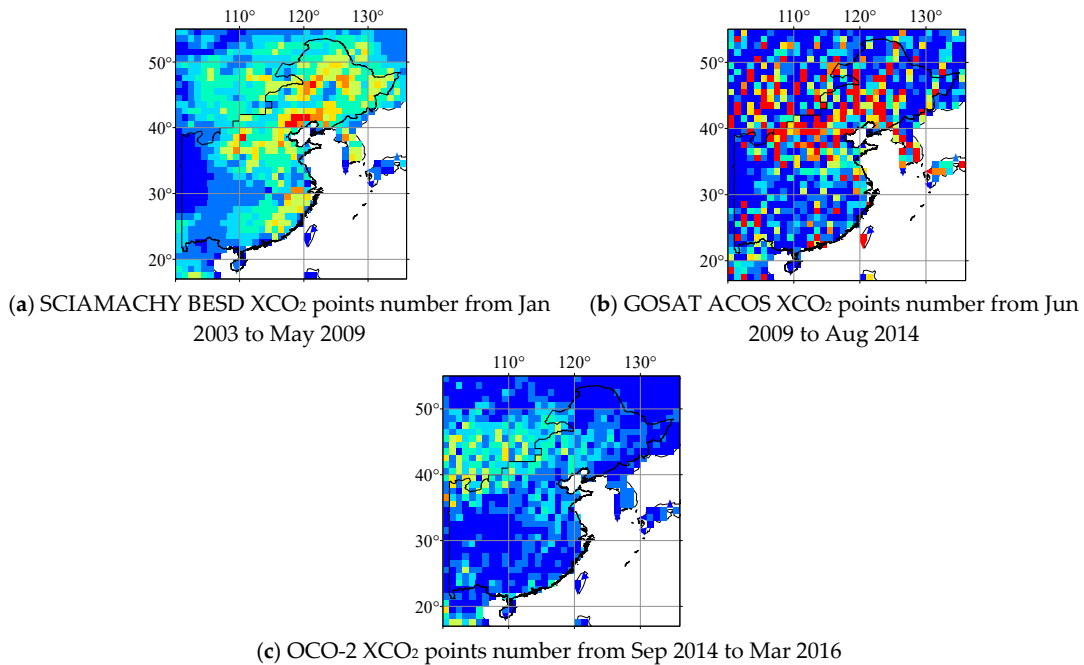

(**a**) SCIAMACHY BESD XCO_2 points number from Jan 2003 to May 2009

(**b**) GOSAT ACOS XCO_2 points number from Jun 2009 to Aug 2014

(**c**) OCO-2 XCO_2 points number from Sep 2014 to Mar 2016

Figure S11. Points number in each grid of integrated satellite observed XCO_2 for SCIAMACHY BESD XCO_2 from Jan 2003 to May 2009 (a), GOSAT ACOS XCO_2 from Jun 2009 to Aug 2014 (b), and OCO-2 XCO_2 from Sep 2014 to May 2016 (c). Study area of eastern China is shown with red edge.
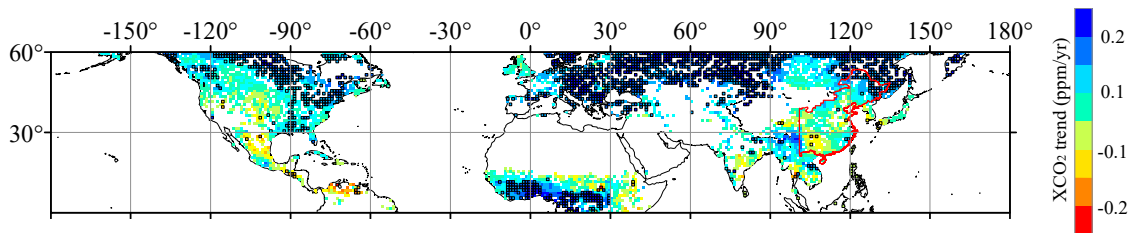
Figure S12. XCO_2 trends in the dormant season, which is defined as times outside the GP, after XCO_2 background increase is removed by CT-XCO_2 fitting. Red grids indicate XCO_2 decrease and blue grids indicate XCO_2 increase. Grids with black outlines indicate the trend is significant (Mann-Kendal test, p<0.05). Study area of eastern China is shown with red edge.

Table 1. CO_2 yearly increase from NOAA global mean, fitted NOAA global mean, global mean from CarbonTracker XCO_2 (CT-XCO_2) fitted results, Mauna Loa site and MLO fitted results. Equation (2) was applied in yearly fitting of all these dataset. Differences between NOAA fitted/CT-XCO_2 fitted results and NOAA global mean (Diff 1 and 2), and differences between MLO fitted results and site yearly increase (Diff 3) were used for check the availability of the fitting method in calculating CO_2 yearly increase.

Year \Growth	NOAA	NOAA Fitted	Diff 1	CT-XCO_2 Fitted	Diff 2	MLO	MLO Fitted	Diff 3
2003	2.29	2.39	0.08	2.23	-0.08	2.27	2.33	0.06
2004	1.57	1.31	-0.24	1.58	0.03	1.60	1.46	-0.14
2005	2.43	2.40	-0.04	2.42	-0.02	2.54	2.41	-0.13
2006	1.75	1.66	-0.11	1.76	-0.01	1.68	1.54	-0.14
2007	2.09	2.18	0.09	2.14	0.05	2.27	2.54	0.27
2008	1.79	1.79	0.01	1.55	-0.23	1.57	1.61	0.04
2009	1.61	1.28	-0.34	1.87	0.25	2.02	2.01	-0.01
2010	2.43	2.94	0.50	2.27	-0.17	2.32	1.94	-0.38
2011	1.70	1.90	0.22	1.74	0.06	1.92	1.63	-0.29
2012	2.39	2.33	-0.05	2.31	-0.07	2.61	2.48	-0.13
2013	2.41	2.11	-0.31	2.40	-0.02	2.01	2.18	0.17
2014	2.04	2.03	-0.02	2.04	-0.01	2.18	2.05	-0.13
2015	2.94	2.34	-0.60	2.70	-0.24	3.02	2.78	-0.24
2016	2.86	3.05	0.21	2.92	0.08	2.99	3.20	0.21
Statistic			-0.04 ± 0.27		-0.03 ± 0.13			-0.06 ± 0.19